



HAL
open science

Lagged rejuvenation of groundwater indicates internal flow structures and hydrological connectivity

Tamara Kolbe, Jean Marçais, Jean-Raynald de Dreuzy, Thierry Labasque,
Kevin Bishop

► **To cite this version:**

Tamara Kolbe, Jean Marçais, Jean-Raynald de Dreuzy, Thierry Labasque, Kevin Bishop. Lagged rejuvenation of groundwater indicates internal flow structures and hydrological connectivity. *Hydrological Processes*, 2020, 34 (10), pp.2176-2189. 10.1002/hyp.13753 . insu-02529125

HAL Id: insu-02529125

<https://insu.hal.science/insu-02529125>

Submitted on 2 Apr 2020

HAL is a multi-disciplinary open access archive for the deposit and dissemination of scientific research documents, whether they are published or not. The documents may come from teaching and research institutions in France or abroad, or from public or private research centers.

L'archive ouverte pluridisciplinaire **HAL**, est destinée au dépôt et à la diffusion de documents scientifiques de niveau recherche, publiés ou non, émanant des établissements d'enseignement et de recherche français ou étrangers, des laboratoires publics ou privés.



Distributed under a Creative Commons Attribution 4.0 International License



Lagged rejuvenation of groundwater indicates internal flow structures and hydrological connectivity

T. Kolbe^{1,2*}, J. Marcais^{3,4}, J.-R. de Dreuzy^{5,6}, Thierry Labasque⁵ and K. Bishop¹

¹ Department of Aquatic Sciences and Assessment, Swedish University of Agricultural Science, 75007 Uppsala, Sweden;

² Section of Hydrogeology and Hydrochemistry, Institute of Geology, Faculty of Geoscience, Geoengineering and Mining, TU Bergakademie Freiberg, 09599 Freiberg, Germany;

³ Institut de Physique du Globe de Paris, Université de Paris, 75005 Paris, France;

⁴ INRAE, UR RiverLy, 69625 Villeurbanne, France;

⁵ Centre National de la Recherche Scientifique (CNRS), Géoscience Rennes - UMR 6118, Université de Rennes, 35042 Rennes, France;

⁶ Centre National de la Recherche Scientifique (CNRS), Institut National de la Recherche Agronomique (INRA), Observatoire des Sciences de l'Univers de Rennes (OSUR) - UMR 3343, Université de Rennes, 35042 Rennes, France;

*Corresponding author: Tamara Kolbe (Tamara.Kolbe@geo.tu-freiberg.de)

Keywords: groundwater age stratification, groundwater recharge, subsurface hydrological connectivity, CFCs, hillslope storage Boussinesq equations, Krycklan, subsurface discharge

This article has been accepted for publication and undergone full peer review but has not been through the copyediting, typesetting, pagination and proofreading process which may lead to differences between this version and the Version of Record. Please cite this article as doi: 10.1002/hyp.13753

Abstract

Large proportions of rain water and snowmelt infiltrate into the subsurface before contributing to stream flow and stream water quality. Subsurface flow dynamics steer the transport and transformation of contaminants, carbon, weathering products and other biogeochemistry. The distribution of groundwater ages with depth is a key feature of these flow dynamics. Predicting these ages are a strong test of hypotheses about subsurface structures and time varying processes. CFC-based groundwater ages revealed an unexpected groundwater age stratification in a 0.47 km² forested catchment called Svartberget in northern Sweden. An overall groundwater age stratification, representative for the Svartberget site, was derived by measuring CFCs from 9 different wells with depths of 2 m to 18 m close to the stream network. Immediately below the water table, CFC-based groundwater ages of already 30 years that increased with depth were found. Using complementary groundwater flow models, we could reproduce the observed groundwater age stratification and show that the 30 year lag in rejuvenation comes from return flow of groundwater at a subsurface discharge zone that evolves along the interface between two soil types. By comparing the observed groundwater age stratification with a simple analytical approximation, we show that the observed lag in rejuvenation can be a powerful indicator of the extent and structure of the subsurface discharge zone, while the vertical gradient of the age-depth relationship can still be used as a proxy of the overall aquifer recharge even when sampled in the discharge zone. The single age stratification profile measured in the discharge zone, close to the aquifer outlet, can reveal the main structure of the groundwater flow pattern from recharge to discharge. This groundwater flow pattern provides information on the participation of groundwater in the hydrological cycle and indicates the lower boundary of hydrological connectivity.

1 Introduction

The time water has spent in a catchment gives information on hydrological processes, solute transport and chemical reactions along flow paths. While a large proportion of stream water measured at the outlet is young, with a mean age of 3 months (Jasechko *et al.*, 2017), water stored in a catchment is much older with ages of weeks for local flow systems and ages of millions of years for regional flow systems (Gleeson *et al.*, 2016; Berghuijs and Kirchner, 2017; Gabrielli *et al.*, 2018). Water ages increase rapidly with depth and longer flow paths that follow the structure of the aquifer and connections to the surface (Vogel, 1967; Cardenas, 2007). Dating stream water at the outlet informs catchment hydrology about catchment functioning at short timescales, but groundwater dynamics at larger timescales are often unseen either due to the choice of tracers or the small portion of older groundwater in the stream. The groundwater age (the time a water parcel has spent in the aquifer from the recharge location at the water table to the sampling location) provides complementary information on the subsurface hydrological cycle including water origin, flow paths, storage capacity and water quality (Haitjema, 1995; Kazemi *et al.*, 2006). When measuring groundwater ages in wells, ages can provide access to some overall features of the groundwater flow dynamics through adapted inference methods, e.g. Lumped Parameter Models (LPM) that have been developed to extract invaluable information from point-like age data (Maloszewski and Zuber, 1996; Jurgens *et al.*, 2012; Åkesson *et al.*, 2015; Marçais *et al.*, 2015; Kolbe *et al.*, 2016). Used within the right concept of flow structures, the points with dated groundwater are useful proxies of difficult-to-access groundwater dynamics. With more cost-effective access to chemical analysis, age data are increasingly measured in well networks, thus giving information on spatial patterns and stratification of ages (Cook *et al.*, 1995; Ayraud *et al.*, 2008; Visser *et al.*, 2009; Gerber *et al.*, 2018). Upslope, age stratifications give useful information on localized recharge and heterogeneity patterns (McMahon *et al.*, 2011). Downslope, closer to discharge from the aquifer to surface water, age stratifications are still influenced by the recharge conditions, but also by the overall aquifer structure. The subsurface to surface interactions become also more intense close the outflow boundary making inferences even more complex (Modica *et*

al., 1998). Groundwater ages at downslope locations conceptually bear information on groundwater dynamics from recharge to discharge, but is it possible to resolve key groundwater characteristics (recharge, aquifer structure, surface/subsurface interactions) from such age data? What is the information content of downslope groundwater ages measured close to the outflow into the surface water network? Are they more influenced by the recharge from further upslope or by the closer downslope discharge? How can these be interpreted? Could an age stratification be reconstructed from different locations or should it be strictly determined from sampling at different depths at the same location? How much should an age stratification be resolved to be useful?

Answers to these practical and fundamental questions are necessary to use downslope age patterns to inform the groundwater dynamics and their interaction with surface and shallow subsurface flows. In an unconfined aquifer, the age T at depth z is theoretically independent of the horizontal location and only related to the volume to recharge ratio as given by

$$T = \frac{\theta H}{R} \ln\left(\frac{H}{H-z}\right) \quad (\text{Eq. 1})$$

with a uniform recharge R , a constant thickness H , and an homogeneous porosity θ (Eq. 1, Vogel, 1967). Recharge processes rejuvenate groundwater at the water table. Under the assumptions that the horizontal extent of the aquifer is much larger than its vertical extent, and that the horizontal velocities are decreasing logarithmically with depth, this will result in an aging of groundwater while circulating deeper into the aquifer. Under such idealized conditions, the age stratification can be reconstructed from any sampling locations of the aquifer far enough from the water divide and the discharge zone. At single locations or transects in recharge zones, groundwater ages at different depths have indeed been proven to follow the expected logarithmic increase with depth in several hydrogeological settings. There, groundwater ages are governed by only a few parameters and Eq. 1 can be used to estimate recharge volumes (Harrington *et al.*, 2002; McMahon *et al.*, 2011; Gates *et al.*, 2014; Kozuskanich *et al.*, 2014).

Investigations on the distribution of groundwater ages within unconfined aquifers have shown the impact of geological heterogeneities (e.g. aquifer properties and structures) and boundary conditions (e.g. groundwater recharge or artificial drainage networks) on the age-depth-

relationship (Cook and Böhlke, 2000; Böhlke, 2002; Jurgens *et al.*, 2012; Leray *et al.*, 2012). Jiang *et al.* (2010) investigated the impact of exponentially decreasing hydrogeological parameters, like in hard-rock aquifers, on age stratifications by numerical modeling and could show that groundwater ages increase with depths in recharge zones while a rejuvenation near the discharge zones takes place. Field and modeling investigations in aquifers with additional artificial heterogeneities, such as drainage networks that are often found in agricultural areas, indicate that relatively old groundwater ages evolve at shallow depths. In such cases, artificial heterogeneities have been found to have a stronger impact on age stratifications than aquifer scale heterogeneity or non-uniform groundwater recharge (Broers, 2004). Dunkle *et al.* (1993) demonstrate by field measurements that the vertical age-depth gradients are smaller and the groundwater ages at the water table are larger in discharge areas, confined zones and areas with a low hydraulic gradient than in recharge areas. This is due to restricted groundwater recharge in these locations, a feature that has been also observed by other authors (Böhlke *et al.*, 2002). Non-uniform recharge conditions have been numerically investigated by Cook and Solomon (1997). Results show that the age stratification is perturbed in areas without recharge, resulting in increased groundwater ages at the water table. Such age stratifications with older groundwater ages at the water table are known as lagged systems and display a discontinuous rejuvenation of groundwater at the water table (Leray *et al.*, 2016). As the types and changes of land use, topography, and soil types influence groundwater recharge, these factors also influence the groundwater age stratification (Houben *et al.*, 2014; Schwarz *et al.*, 2018).

Leray *et al.* (2016), Jurgens *et al.* (2012) and IAEA (2006) summarize some adaptations and further developments of Eq. 1 that have been derived by these observed deviations to approximate groundwater age stratifications. Even with consideration of these factors, it is challenging to estimate the distribution of groundwater ages within aquifers. Nevertheless, we hypothesize that sampling full flowlines at several locations and different depths downslope close to the stream network would provide useful information about overall groundwater flow dynamics. By sampling close to the stream network we expect to get the age of the full flow path. By sampling at different

depths and distances from the stream network, we also expect to get information that can help to estimate the recharge volume.

In this study, we investigate the information content of downslope measured groundwater ages and the possibility to single out key groundwater characteristics (recharge, aquifer structure, surface/subsurface interactions). Sampling locations were chosen from existing wells at the Svartberget study site, a subcatchment of the Krycklan catchment in northern Sweden. Sampling locations were already existing and located downslope with different depths and not necessarily on the same transect. We explored the overall groundwater age pattern and revealed underlying information on recharge and discharge processes by applying a numerical groundwater flow model. By comparing our measured groundwater age stratification with a simple analytical approximation, we demonstrate how this overall age stratification gives insights into the groundwater flow dynamics from recharge to discharge locations. These insights are the basis for further defining the lower boundary for water taking part in the local hydrological cycle, a proxy for the subsurface hydrological connectivity. These insights are also useful for understanding biogeochemical fluxes and their impact on water quality at the catchment scale.

2 Study site

2.1 General description

The study site Svartberget ($64^{\circ}14'N$, $19^{\circ}46'E$, 0.47 km^2) is located in the long-term research catchment Krycklan, one of the most instrumented and monitored catchments in the world (Laudon *et al.*, 2013). Hydrometric data and water stable isotopes are recorded at the outlet and monitoring wells. The topography ranges from 234 m to 306 m with a mean elevation of 274 m and is characterized by gentle slopes (Fig. 1). The climate is cold and humid with a mean temperature of 1.8°C . The average period of snow cover is 168 days; the mean precipitation is 614 mm/a and mean runoff is 321 mm/a (Laudon *et al.*, 2013). There are two stream channels within the study site that were deepened during the 1910s to improve forest drainage. The main channel, Kallkällbäcken, originates from a mire that covers 18% of the area. The other channel,

Västrabäcken, goes parallel to it and they merge close to the outlet (C7) of the Svartberget study site. Besides the open mire area, the vegetation cover consists of pine and spruce forest (82% of the area) (Fig. 1). Regarding the soil types, 65% of the area is covered by glacial till, 18% by peat and 16% by thin soils. Geophysical methods have shown that the soil depth varies between 0 m and 22 m with a mean depth of 11.5 m to the bedrock (Lindqvist *et al.*, 1989). Within the glacial till that covers the bedrock a distinction between the dense basal till nearest the bedrock and the shallow ablation till up to 3 m depth has to be made (Nyberg *et al.*, 2001). The shallow ablation till, with a higher hydraulic conductivity than the dense basal till, is primarily transmitting the water in the subsurface (Pinder and Celia, 2006). The bedrock is gneiss (meta-greywache) and poorly weathered (Grabs *et al.*, 2009). The bedrock contains horizons of biotite-plagioclase and graphite-sulphide schists (Mason, 1991).

2.2 Hydrological functioning

Investigations on the hydrological functioning of the Svartberget site have been undertaken since 1980 by combinations of hydrometric and water stable isotope methods as well as modeling tools (Bishop *et al.*, 1990; Laudon *et al.*, 2007, 2013, Peralta-Tapia *et al.*, 2015b, 2015a; Karlsen *et al.*, 2016; Ledesma *et al.*, 2018b). Studies have shown that stream water consists of over 80% to 90% of pre-stored water due to flashy responses from glacial till soils (Rodhe, 1989). The high proportions of pre-stored water in stream water is congruent with mass balance calculations based on the distribution of catchment storages, water fluxes and flow paths (Amvrosiadi *et al.*, 2017). Within hours of rainfall or snowmelt, a rapid transmission of pre-stored water with dynamically varying chemical properties to the stream has been observed. Researchers explain this behavior by the concept of transmissivity feedback (Bishop, 1991). A transmissivity feedback evolves due to an increase of the saturated hydraulic conductivity towards the surface. When the water table rises and reaches the higher hydraulic conductivities, the rise of the water table slows down and water flows within the shallow permeable layer to the stream. At Svartberget ablation till with higher hydraulic conductivities has been observed up to 3 m depth below the land surface at the water

divide (Nyberg *et al.*, 2001). When the layer with higher hydraulic conductivities gets activated, shallow subsurface flow spends in average not longer than 2 years in the subsurface (Amvrosiadi *et al.*, 2017). Streams are strongly incised (sometimes due to human intervention to increase drainage in the headwater catchments) and the transiently activated permeable layer transmits most of the annual flow primarily during periods of high flow, e.g. in spring during snowmelt. Little overland flow has been observed at the site even during high flow seasons, because of the high infiltration capacity of the till (Rodhe, 1989). It has been shown that water table elevations and stream discharge are strongly correlated providing some insights into the runoff generation and the export of solutes (Bishop *et al.*, 2004; Ameli *et al.*, 2016; Ledesma *et al.*, 2018a). All these findings provide insights on the hydrological functioning on the timescale of month to a few years, but little is known about the groundwater dynamics beyond a few years, the groundwater that flows in the less permeable layer. But especially this water sustains low flows in streams, and in fact defines the chemistry of stream flow during most of the year (Ledesma *et al.*, 2013). Little is known about flow structures from groundwater recharge to discharge zones and the vertical extent of groundwater taking part in the hydrological cycle. Quantifying the age of this water is crucial for weathering and biogeochemical reactions as well as for determining the export of nutrients and weathering products from the aquifer.

3 Methods

3.1 Chlorofluorocarbon measurements and determination of apparent groundwater ages

Depending on the timescale of groundwater flow dynamics, an appropriate age tracer has to be selected to date groundwater (Kazemi *et al.*, 2006). Chlorofluorocarbons (CFCs) as atmospheric tracers have been widely used to date groundwater up to some decades and to infer aquifer characteristics. It is assumed that CFC concentrations are in equilibrium with the atmosphere above the water table for unsaturated zones of less than 5 m (Engesgaard *et al.*, 2004; Schwientek *et al.*, 2009) before being recharged in the aquifer by recharge processes and further transported conservatively with groundwater flow. A comparison among the measured CFCs (CFC-11, CFC-

12 and CFC-113) gives insight into their conservative nature and potential degradation, sorption or contamination. The limitations of this tracer are extensively discussed in Busenberg and Plummer (1992) and Cook and Solomon (1997).

We collected groundwater samples at specific depths in 9 individual sampling locations in till soils within the Svartberget study site in September 2017 (Fig. 1). The specific sampling depths covered sampling intervals of maximum 1 m ranging from the water table to a depth of 16.7 m below the water table and were located in the basal till below the lowest observed water table (Appendix, Tab. A1). All sampling locations are downslope with distances of 20 m and 80 m from the stream network. The unsaturated zone thickness measured at the sampling locations was between 0.9 m and 2.7 m. CFC concentrations were analyzed at the OSUR analytical platform “CONDATE Eau” at the University of Rennes in France. By sampling flowlines at given depths, we assume sampling of flowlines with consistent groundwater ages. By knowing the atmospheric CFC concentrations in time and the concentration in the sample, we can determine the recharge year and therefore calculate the apparent age of our sample (Kazemi *et al.*, 2006).

3.2 Conceptual subsurface flow

The shallow ablation till layer with higher hydraulic conductivities that transmits most of the water and the denser basal till layer with lower hydraulic conductivities below give evidence for the subsurface structure being a two layered system (Jutebring Sterte *et al.*, 2018). At the sampling date, the water table and stream discharge were low, which testifies that the shallow permeable layer was not being fully activated. At locations downslope where the less permeable layer was fully saturated and therefore the shallow permeable layer activated, i.e. groundwater was discharging from the less permeable to the shallow permeable layer. Groundwater flow mainly occurred in the less permeable layer. When it rains the shallow permeable layer is activated as soon as the water table rises up to this layer and water is transmitted laterally to the stream. The hydraulic conductivity and porosity within each of the two layers are assumed to be homogenous

as there are no other specific geological irregularities observed besides the decline in hydraulic conductivity with depth. The fresh bedrock is assumed to be impermeable and flat.

3.3 Simulation of groundwater ages

We simulated groundwater flow and transport using the hillslope storage Boussinesq equations that have been further developed to account for a two-layered system with return flow (Marçais *et al.*, 2017). The interface between the two layers (shallow permeable and deep less permeable layer) has been interpolated from field information, i.e. geophysical measurements (Lindqvist *et al.*, 1989). The hillslope storage Boussinesq equations yield a 1D approximation of the subsurface flow by integrating the discharge transversally to the slope direction. The discharge is proportional to the width of the transect profile. The simulation of transport is performed in 2D (Strack, 1984; Pollock, 1988; Harman and Kim, 2019). We applied the equations to a representative hillslope that has been generated from a DEM with a resolution of 5 m by taking all cells with the same distance to the stream and calculating a mean elevation, and the corresponding width (Fig. 2). The width function was fitted by a typical exponential function to prevent local seepage formations not representative of catchment scale connectivity (Troch *et al.*, 2002).

An annual mean infiltration of 321 mm (mean net-precipitation from 1981 till 2017) is taken to simulate steady-state groundwater flow and applied to the top of the model domain. The hydrogeological parameters (i.e. porosity and hydraulic conductivity) are assigned to each of the two layers. Regarding the well-studied shallow permeable layer, it has been shown that the hydraulic conductivity follows an exponential decrease with depth. In the simplified two-layered system, a homogeneous porosity of 0.4 and homogeneous hydraulic conductivity of 22.88 m/d have been assigned. These values represent mean values for a mean thickness of the permeable layer of 1.5 m (Bishop, 1991; Nyberg *et al.*, 2001; Ameli *et al.*, 2016; Amvrosiadi *et al.*, 2017). The homogeneous porosity and homogeneous hydraulic conductivity of the deeper less permeable layer are calibrated against CFC-12 concentrations (see 4.1) measured in different wells covering a variety of depths and distances to the stream (see Fig. 2 showing the different depths and distance

to the stream network). The MATLAB built-in function `fminsearch` (Lagarias et al., 1998) is used to minimize the objective function $\Phi(k, \theta)$:

$$\Phi(k, \theta) = \frac{\sum_{i=1}^9 |C_{CFC_i}^{mod}(k, \theta, x_i, z_i) - C_{CFC_i}^{obs}(x_i, z_i)|}{\sum_{i=1}^9 C_{CFC_i}^{obs}(x_i, z_i)} \quad (\text{Eq. 2})$$

where k and θ are respectively the hydraulic conductivity and the porosity of the less permeable layer in the model, C_{CFC}^{mod} is the modelled CFC-12 concentration and C_{CFC}^{obs} the measured CFC-12 concentration at a depth z_i from the water table and at a distance x_i from the stream for the nine different sampling locations. Modelled CFC-12 concentrations are derived by convoluting the historical CFC-12 atmospheric concentrations C_{CFC}^{in} with the residence time distribution p_{RT} for each of the sampling locations (Eq. 3 and 4).

$$C_{CFC}^{mod}(t, mRT, \alpha, \lambda) = \int_0^{+\infty} C_{CFC}^{in}(t-u) p_{RT}(u, mRT, \alpha, \lambda) du \quad (\text{Eq. 3})$$

with

$$p_{RT}(t, mRT, \alpha, \lambda) = \left(\frac{mRT \lambda}{4\pi\alpha t^3}\right)^{1/2} \exp\left(-\frac{(t-mRT)^2 \lambda}{4\alpha mRT t}\right) \quad (\text{Eq. 4})$$

where α is the dispersivity (in m), λ is the traveled distance of the particle and mRT the mean residence time of the particles. α is assumed to be equal to 0.1λ (Gelhar, 1992). mRT and λ depends on the hydraulic conductivity k and of the porosity θ chosen for the simulation but also depends on the sampling location (x_i, z_i) .

Each modeled groundwater age represents the mean residence time from the calibrated model. The calibrated model is then used to show the distribution of groundwater ages within the representative hillslope and to determine the groundwater recharge volume to the less permeable layer. A sensitivity analysis, presented in the discussion section, shows how the infiltration rate impacts the partitioning of the amount that discharges through the shallow permeable layer and the deeper less permeable layer, as well as resulting distributions of groundwater ages.

4 Results

4.1 Measured CFC-based groundwater ages

The CFC-based groundwater ages presented here are based on CFC-12 measurements. All of the CFC-based groundwater ages were compared among each other to evaluate their conservative behavior. The comparison revealed differences in ages of less than 7 years between the CFCs. CFC-11 based groundwater ages were higher than CFC-12 and CFC-113 based groundwater ages (see Appendix, Tab. A1). This pattern has been typically observed in environments with microbial degradation and is supported by the anoxic conditions at the site (Dunkle *et al.*, 1993; IAEA, 2006). As CFC-12 is known to be less reactive than CFC-11 and CFC-113, the CFC-12 based groundwater ages are taken here as the most reliable groundwater ages and the ones chosen for use in the rest of this study. An ambiguous interpretation of CFC-12 concentrations with respect to the peak in atmospheric concentrations can be precluded, as determined concentrations indicated ages older than this range around the peak. CFC-12 based groundwater ages are between 30 and 56 years (Fig. 3; Appendix, Tab. A1). Close to the water table, the groundwater ages are already 30 years. This is a deviation from the expected natural stratification that starts with groundwater ages close to zero at the water table. Groundwater ages then increase up to 54 years at around 16 m below the water table. Although the samples were taken at different locations at the Svartberget site, they follow a similar age-depth-relationship. This suggests a single overall groundwater age stratification for the study site.

4.2 Simulated groundwater ages

CFC-12 concentrations were used to calibrate groundwater flow and to derive the distribution of groundwater ages (representing mean residence times for each sampling point) within the representative hillslope (Appendix, Tab. A2). The residual of the optimization procedure is 0.16. Simulated groundwater ages are presented between 20 m and 80 m distance to the stream, the distances to the stream in which the 9 sampling locations are located. The steady-state simulation

of groundwater ages matches best the behavior of measured CFC-based groundwater ages by applying a hydraulic conductivity of 0.213 m/d and a porosity of 0.28 for the less permeable layer (Fig. 4). Within the distance of 20 m to 80 m to the stream, simulated groundwater ages at the water table show a lag of rejuvenation represented in groundwater ages of around 46 years at 20 m distance and 30 years at 80 m distance, respectively. By plotting the age stratification at these distances, the simulated groundwater ages follow the same trend (increase of groundwater ages with depth) as the measured groundwater ages. The simulated groundwater ages at 20 m distance are older than the simulated groundwater ages at 80 m. This is also in accordance with measured groundwater ages, e.g. groundwater ages closer to the stream are older than the ones further away considering groundwater ages measured at a similar depth.

In Fig. 5 the distribution of groundwater ages within the saturated zone of the representative hillslope and the groundwater ages at the water table are shown. For distances larger than 250 m, the less permeable layer is not fully saturated. Here, the water table is below the shallow permeable layer. Groundwater recharge rejuvenates groundwater ages with zero groundwater ages at the water table that increase with depth. At distances between 0 - 250 m to the stream, the less permeable layer is fully saturated and prevents infiltration. The saturated thickness in the shallow permeable layer is 15 cm on average, with a maximum thickness of 35 cm. A subsurface discharge zone develops, where groundwater discharges from the less permeable layer to the shallow permeable layer. In this area groundwater recharge to the less permeable layer does not take place and groundwater ages get older when moving closer to the stream. Due to the extent of the subsurface discharge zone (0 – 250 m distance from the stream), only 1/3 (109 mm/a) of the applied infiltration rate of 321 mm/a recharges the groundwater in the less permeable layer. 2/3 of the applied infiltration rate remains in the shallow permeable layer and is transmitted to the stream.

5 Discussion

5.1 Informative content of downslope measured groundwater age stratification

In unconfined aquifers a natural age stratification with groundwater ages that logarithmically increase with depth exists (Vogel, 1967). At our study site, we could assemble an overall age stratification from different sampling locations located downslope near the stream network. The impact of the stream boundary seems negligible at these distances as an age stratification could be preserved. Nevertheless, influenced by recharge and discharge processes, we observe a deviation from the expected natural age stratification with groundwater ages of around 30 years close to the water table that increases with depth. Groundwater ages of 30 years at the water table indicate a lag of rejuvenation. Reasons for such a lag can be the aquifer structure (e.g. confined conditions) or a thick unsaturated zone, but these have not been observed at the study site. A more plausible explanation for this lag at the Svartberget site is that groundwater ages are not rejuvenated at certain locations. Here, the lag of recharge evolves due to the generation of a subsurface discharge zone that is related to the subsurface structure and the decline of hydraulic conductivity with depth (Fig. 5). The subsurface discharge zone is not obviously visible from topographic and other catchment metrics, but is well constrained by field data and confirmed by our modeling approach as well as other catchment observations. For example, Klaminder *et al.* (2011) investigated the importance of carbon mineralization and pyrite oxidation for silicate weathering at the study site and showed increasing pH, concentration of inorganic C, base cations, SO₄ and Si while O₂ concentrations decreased with increasing distance from the water divide along the hillslope. Infiltrating groundwater would provoke an increase of O₂ concentrations as recharging water is enriched in O₂. Their results promote our hypothesis of groundwater discharge at these locations that prevent infiltration.

For future age tracer interpretations at the site, our findings suggest an exponential piston flow model as the most appropriate LPM for simulating a groundwater age distribution in a fully-screened well located in a discharge zone (Maloszewski and Zuber, 1996; Jurgens *et al.*, 2012).

The downslope age stratification presented here provides inherent information on groundwater dynamics within recharge and discharge, but it is necessary to apply a simple analytical approximation to reveal key characteristics from the measured groundwater age stratification, like the recharge volume or the relation between recharge and subsurface discharge zone. With these two measures we would then not only get information about the recharge volume commonly measured in recharge zones, but we also gain additional information about the connectivity of the groundwater body with the surface, in this study represented by the subsurface discharge zone.

5.2 Interpretation and analytical approximation of groundwater age stratification

There have been numerous age stratifications reported in the literature with the development of analytical solutions to predict and assess age stratifications from a few aquifer parameters. An analytical solution involving a subsurface discharge zone, such as we do here, has not yet been reported. The generation of a discharge zone prevents water from infiltrating into the aquifer, acting like a confinement at this location (Fig. 6A) (IAEA, 2006). Thus we propose to apply an analytical solution for lagged systems described as aquifer systems where the aquifer type changes from unconfined to confined conditions (Fig. 6B). The groundwater ages at any location in the area where subsurface discharge occurs depends on the characteristics of both, the unconfined part and the “confined” part of the aquifer. In our case this is the part where the subsurface discharge zone develops. The controlling parameters are the area of the recharge zone A_r and the area of the discharge zone A_d , together with the thickness of the aquifer H , the groundwater recharge R as well as porosity θ of the geological medium that determines the slope of the age-depth relationship. The analytical approximation demonstrates that the ratio between the area of recharge zone and the area of the discharge zone A_d/A_r can be obtained by the observed mean groundwater age related to the discharge zone $\tau_{d,obs}$ of 31 years divided by the observed mean groundwater age related to the recharge zone $\tau_{r,obs}$ of 26 years (Fig. 6C). Measured groundwater ages indicate a ratio of A_d/A_r of 1.2. Comparing this result to our model results with a modelled discharge area of 0.3 km² and a

modelled recharge area of 0.2 km^2 ($A_d/A_r = 1.5$), shows that the A_d/A_r ratio can be obtained by the observed groundwater ages with an error of 20 %.

When applying the analytical solution for lagged systems just a few aquifer characteristics are needed to get a first estimate of the aquifer functioning. To fit the analytical solution to measured groundwater ages, the observed groundwater age stratification has to be resolved to a certain extent meaning that measurements close to the water table and along the full depth of the aquifer are necessary. Deviations from the analytical solution might be due to heterogeneities in the subsurface or recharge.

5.3 Impact of infiltration rates on groundwater age stratification

The aquifer is exposed to strong seasonal changes with a variation of infiltration rates affecting subsurface flow. Here, we present a sensitivity analysis on the infiltration rate. While this is not a substitute for a fully transient simulation, it still clearly shows the potential impact of the partitioning of the infiltration rate into the amount that discharges through the shallow permeable layer and the deeper less permeable layer. The aquifer receives high volumes of water during snowmelt in spring. In summer and winter there is less infiltration due to less rainfall and snow accumulation on the surface. Intermediate infiltration occurs during autumn due to occasional rainfall events (Karlsen *et al.*, 2016). Considering these extreme variations in infiltration rates, the connection between the shallow permeable layer and the less permeable layer vary to a certain extent.

Additional simulations with a lower (146 mm/a for winter) and higher (840 mm/a for spring) infiltration rate demonstrate how much water actually recharges to the deeper less permeable layer and how the subsurface discharge zone, i.e. connection between the shallow permeable layer and less permeable layer, changes compared to the reference model with a mean annual infiltration of 321 mm/a (Fig. 7 and Tab. 1). Higher infiltration rates raise the water table and increase the extent of the discharge zone, which can be observed in higher groundwater ages at the water table at our sampling locations (Fig. 7 and Tab. 1). Due to the extension of the subsurface discharge zone, the

area of the recharge zone decreases and a smaller fraction of the infiltration recharges to the less permeable layer than was the case in the reference model. The actual amount of groundwater recharge is higher for the spring model than for the reference model (Tab. 1). This results in a less steep slope of the age-depth-relationship, meaning that groundwater age increases more slowly with depth than for the reference model. By applying a lower infiltration rate, the water table falls and the subsurface discharge zone decreases. Thus a higher fraction of the infiltration recharges to the less permeable layer than for the reference model. The actual amount of groundwater recharge is less for the winter model than for the reference model (Tab. 1). Due to a decrease of the subsurface discharge zone, the recharge zone of the less permeable layer increases (Fig. 7 and Tab. 1). The lag of rejuvenation decreases as the area where groundwater recharges to the less permeable layer increases. The slope of the age-depth-relationship gets steeper, meaning that groundwater age increases faster with depth than for the reference model, due to the decreased groundwater recharge to the less permeable layer. These results demonstrate the importance of considering the partitioning of the infiltration amount and pose a limitation for estimating a mean groundwater age T_{mean} only from an estimated groundwater recharge value R by knowing the thickness of the saturated zone H and the porosity θ ($T_{mean} = \frac{\theta H}{R}$).

5.4 Relevance beyond our study site

By analyzing a single overall groundwater age stratification from downslope sampling locations, the extent of groundwater contributing to the hydrological cycle can be defined. Connections of the deep groundwater with the surface can be informed by extracting the vertical slope of the age-depth-relationship that provides information about the recharge volume. Connectivity between the deep groundwater in the less permeable layer and the shallow groundwater in the shallow permeable layer can be defined by extracting the lag of rejuvenation that indicates the extent of the discharge zone in relation to the recharge zone. Overall, the distribution of ages with depths marks the vertical hydrological connectivity, i.e. timescales and related depths taking part in the local hydrological cycle. This is an important measure for hydro(geo)logists, ecologists, and water

resource managers as the transport of water, including the division into local flow systems that discharge to the nearest watercourse, and regional groundwater flow systems, has implications for the transport of contaminants, chemical weathering and biogeochemical fluxes (Maher and Chamberlain, 2014; Erlandsson *et al.*, 2016).

In general, hydrological connectivity has been described as “the water mediated transport of matter, energy and organisms within or between hydrological elements of the hydrological cycle” (Ali *et al.*, 2018; Bracken & Croke, 2007), but depending on the researcher’s background and spatial as well as temporal scale of investigation this term has been adapted as no universal definition exists (Michaelides and Chappell, 2009). Nevertheless, researchers agree that hydrological connectivity can be separated into structural connectivity (structure of the subsurface, i.e. spatial distribution of hydrogeological parameter or lithology) and functional connectivity (description of process, i.e. flow or type of boundary conditions) that are mutually dependent (Renard and Allard, 2013). Speaking in terms of structural and functional connectivity related to our findings, we clearly observe a strong control of the processes (functional connectivity) occurring at the Svartberget site. The subsurface discharge zone generates a lag of rejuvenation that impacts the recharge volume to the less permeable layer and vice versa.

Such a subsurface discharge zone is not only relevant at the Svartberget site. The decline in hydraulic conductivity with depth that led to this subsurface process has been found in many other environments. These include weathered and fractured media as well as porous media (Jiang *et al.*, 2009), in glacial till catchments (Nyberg, 1995; Grip, 2015), and in forested catchments, as the increased root density can increase the efficiency of preferential flow paths forming a near surface permeable zone (Schwarz *et al.*, 2018).

6 Conclusion

In the study, a single overall groundwater age stratification provided spatially and temporally distributed information about the groundwater recharge and discharge relationship. By measuring groundwater ages downslope from different sampling locations we derive a specific age vs depth

relationship that is distinct from other studies and provides useful insights on groundwater dynamics. We emphasize two measures extracted from the groundwater age stratification, (1) the lag of rejuvenation that indicates the extent of the subsurface discharge zone in relation to the recharge zone. Here, the discharge zone acts as a confinement of the aquifer and hinders aquifer recharge. (2) The increase of ages with depth yields information about the recharge volume.

At our site this lag of rejuvenation is due to a hydrodynamic effect, the generation of the subsurface discharge zone, which evolves between a highly permeable to less permeable subsurface layer. The 2-layered system originates from the subsurface structure, the strong decline in hydraulic conductivity with depth, which is a common feature not specific to our study site. This has been observed in various other locations, suggesting that the findings here are also applicable to other sites. This subsurface discharge zone might especially occur in catchments that are characterized by till soils or in other catchments with rapid changes of hydraulic conductivity with depth.

By selecting a simple analytical approximation for this groundwater age stratification, we demonstrate a strong capability to infer further information about the aquifer from groundwater age data. These insights provide a basis for linking water and biogeochemical fluxes in groundwater that also affect surface water quality. Furthermore, we elaborate a metric for describing subsurface hydrological connectivity not merely at our study site, but rather as a general tool and for comparison of individual study sites.

Acknowledgments

This project has been funded by the Swedish University of Agricultural Sciences (SLU), Department of Aquatic Sciences and Assessment. Many thanks to the Krycklan catchment study (KCS) group and especially to Hjalmar Laudon and Johannes Tiwari for their help throughout the process. KCS is supported by the Swedish Science Foundation SITES, ForWater, Future Forest, Kempe Foundation and SKB. Many thanks also to Reinert Huseby Karlsen for his support and Anna Nydahl for the pleasant company during the field campaign.

Data Availability Statement

The data that support the findings of this study are available from the corresponding author upon reasonable request.

References

- Åkesson M, Suckow A, Visser A, Sültenfuß J, Laier T, Purtschert R, Sparrenbom CJ. 2015. Constraining age distributions of groundwater from public supply wells in diverse hydrogeological settings in Scania, Sweden. *Journal of Hydrology* **528**: 217–229 DOI: <http://dx.doi.org/10.1016/j.jhydrol.2015.06.022>
- Ali G, Oswald C, Spence C, Wellen C. 2018. The T-TEL Method for Assessing Water, Sediment, and Chemical Connectivity. *Water Resources Research* **54** (2): 634–662 DOI: 10.1002/2017WR020707
- Ameli AA, Amvrosiadi N, Grabs T, Laudon H, Creed IF, McDonnell JJ, Bishop K. 2016. Hillslope permeability architecture controls on subsurface transit time distribution and flow paths. *Journal of Hydrology* **543**: 17–30 DOI: 10.1016/j.jhydrol.2016.04.071
- Amvrosiadi N, Seibert J, Grabs T, Bishop K. 2017. Water storage dynamics in a till hillslope: the foundation for modeling flows and turnover times. *Hydrological Processes* **31** (1): 4–14 DOI: 10.1002/hyp.11046
- Ayraud V, Aquilina L, Labasque T, Pauwels H, Molenat J, Pierson-Wickmann AC, Durand V, Bour O, Tarits C, Le Corre P, et al. 2008. Compartmentalization of physical and chemical properties in hard-rock aquifers deduced from chemical and groundwater age analyses. *Applied Geochemistry* **23** (9): 2686–2707 DOI: 10.1016/j.apgeochem.2008.06.001
- Berghuijs WR, Kirchner JW. 2017. The relationship between contrasting ages of groundwater and streamflow. *Geophysical Research Letters* **44** (17): 8925–8935 DOI:

10.1002/2017GL074962

- Bishop K. 1991. Episodic increases in stream acidity, catchment flow pathways and hydrograph separation. *Ph. D. thesis, Univ. of Cambridge*
- Bishop K, Seibert J, Köhler S, Laudon H. 2004. Resolving the Double Paradox of rapidly mobilized old water with highly variable responses in runoff chemistry. *Hydrological Processes* **18** (1): 185–189 DOI: 10.1002/hyp.5209
- Bishop KH, Grip H, O'Neill A. 1990. The origins of acid runoff in a hillslope during storm events. *Journal of Hydrology* **116** (1–4): 35–61 DOI: 10.1016/0022-1694(90)90114-D
- Böhlke J-K. 2002. Groundwater recharge and agricultural contamination. *Hydrogeology Journal* **10** (1): 153–179 DOI: 10.1007/s10040-001-0183-3
- Böhlke JK, Wanty R, Tuttle M, Delin G, Landon M. 2002. Denitrification in the recharge area and discharge area of a transient agricultural nitrate plume in a glacial outwash sand aquifer, Minnesota. *Water Resources Research* **38** (7): 10-1-10–26 DOI: 10.1029/2001WR000663
- Bracken LJ, Croke J. 2007. The concept of hydrological connectivity and its contribution to understanding runoff-dominated geomorphic systems. *Hydrological Processes* **21** (13): 1749–1763 DOI: 10.1002/hyp.6313
- Broers HP. 2004. The spatial distribution of groundwater age for different geohydrological situations in the Netherlands: implications for groundwater quality monitoring at the regional scale. *Journal of Hydrology* **299** (1–2): 84–106 DOI: 10.1016/j.jhydrol.2004.04.023
- Busenberg E, Plummer LN. 1992. Use of chlorofluorocarbons (CCl₃F and CCl₂F₂) as hydrologic tracers and age-dating tools: The alluvium and terrace system of central Oklahoma. *Water Resources Research* **28** (9): 2257–2283 DOI: 10.1029/92WR01263

- Cardenas MB. 2007. Potential contribution of topography-driven regional groundwater flow to fractal stream chemistry: Residence time distribution analysis of Tóth flow. *Geophysical Research Letters* **34** (5): L05403 DOI: 10.1029/2006GL029126
- Cook PG, Böhlke J-K. 2000. Determining Timescales for Groundwater Flow and Solute Transport. In *Environmental Tracers in Subsurface Hydrology* Springer US: Boston, MA; 1–30. DOI: 10.1007/978-1-4615-4557-6_1
- Cook PG, Solomon DK. 1997. Recent advances in dating young groundwater: Chlorofluorocarbons, H-3/He-3 and Kr-85. *Journal of Hydrology* **191** (1–4): 245–265 DOI: 10.1016/s0022-1694(96)03051-x
- Cook PG, Solomon DK, Plummer LN, Busenberg E, Schiff SL. 1995. Chlorofluorocarbons as tracers of groundwater transport processes in a shallow, silty sand aquifer. *Water Resources Research* **31** (3): 425–434 DOI: 10.1029/94wr02528
- Dunkle SA, Plummer LN, Busenberg E, Phillips PJ, Denver JM, Hamilton PA, Michel RL, Coplen TB. 1993. Chlorofluorocarbons (CCl₃F and CCl₂F₂) as dating tools and hydrologic tracers in shallow groundwater of the Delmarva Peninsula, Atlantic Coastal Plain, United States. *Water Resources Research* **29** (12): 3837–3860 DOI: 10.1029/93WR02073
- Engesgaard P, Højberg AL, Hinsby K, Jensen KH, Laier T, Larsen F, Busenberg E, Plummer LN. 2004. Transport and Time Lag of Chlorofluorocarbon Gases in the Unsaturated Zone, Rabis Creek, Denmark. *Vadose Zone Journal* **3** (4): 1249 DOI: 10.2136/vzj2004.1249
- Erlandsson M, Oelkers EH, Bishop K, Sverdrup H, Belyazid S, Ledesma JLJ, Köhler SJ. 2016. Spatial and temporal variations of base cation release from chemical weathering on a hillslope scale. *Chemical Geology* **441**: 1–13 DOI: 10.1016/J.CHEMGEO.2016.08.008
- Gabrielli CP, Morgenstern U, Stewart MK, McDonnell JJ. 2018. Contrasting Groundwater and

Streamflow Ages at the Maimai Watershed. *Water Resources Research* **54** (6): 3937–3957
DOI: 10.1029/2017WR021825

Gates JB, Steele G V., Nasta P, Szilagyi J. 2014. Lithologic influences on groundwater recharge through incised glacial till from profile to regional scales: Evidence from glaciated Eastern Nebraska. *Water Resources Research* **50** (1): 466–481 DOI: 10.1002/2013WR014073

Gerber C, Purtschert R, Hunkeler D, Hug R, Sültenfuss J. 2018. Using environmental tracers to determine the relative importance of travel times in the unsaturated and saturated zones for the delay of nitrate reduction measures. *Journal of Hydrology* **561**: 250–266 DOI: 10.1016/J.JHYDROL.2018.03.043

Gleeson T, Befus KM, Jasechko S, Luijendijk E, Cardenas MB. 2016. The global volume and distribution of modern groundwater. *Nature Geoscience* **9** (2): 161–167 DOI: 10.1038/ngeo2590

Grabs T, Seibert J, Bishop K, Laudon H. 2009. Modeling spatial patterns of saturated areas: A comparison of the topographic wetness index and a dynamic distributed model. *Journal of Hydrology* **373** (1–2): 15–23 DOI: 10.1016/J.JHYDROL.2009.03.031

Grip H. 2015. Sweden's first forest hydrology field study 1905-1926: contemporary relevance of inherited conclusions and data from the Rokliden Hillslope. *Hydrological Processes* **29** (16): 3616–3631 DOI: 10.1002/hyp.10420

Haitjema HM. 1995. On the residence time distribution in idealized groundwatersheds. *Journal of Hydrology* **172** (1–4): 127–146 DOI: 10.1016/0022-1694(95)02732-5

Harman CJ, Kim M. 2019. A low-dimensional model of bedrock weathering and lateral flow coevolution in hillslopes: 1. Hydraulic theory of reactive transport. *Hydrological Processes* **33** (4): 466–475 DOI: 10.1002/hyp.13360

- Harrington GA, Cook PG, Herczeg AL. 2002. Spatial and Temporal Variability of Ground Water Recharge in Central Australia: A Tracer Approach. *Ground Water* **40** (5): 518–527 DOI: 10.1111/j.1745-6584.2002.tb02536.x
- Houben GJ, Koeniger P, Sültenfuß J. 2014. Freshwater lenses as archive of climate, groundwater recharge, and hydrochemical evolution: Insights from depth-specific water isotope analysis and age determination on the island of Langeoog, Germany. *Water Resources Research* **50** (10): 8227–8239 DOI: 10.1002/2014WR015584
- IAEA. 2006. Use of Chlorofluorocarbons in Hydrology: a guidebook. *International Atomic Energy Agency*: 291
- Jasechko S, Perrone D, Befus KM, Bayani Cardenas M, Ferguson G, Gleeson T, Luijendijk E, McDonnell JJ, Taylor RG, Wada Y, et al. 2017. Global aquifers dominated by fossil groundwaters but wells vulnerable to modern contamination. *Nature Geoscience* **10** (6): 425–429 DOI: 10.1038/ngeo2943
- Jiang XW, Wan L, Cardenas MB, Ge SM, Wang XS. 2010. Simultaneous rejuvenation and aging of groundwater in basins due to depth-decaying hydraulic conductivity and porosity. *Geophysical Research Letters* **37**: 5 DOI: L0540310.1029/2010gl042387
- Jiang XW, Wan L, Wang XS, Ge S, Liu J. 2009. Effect of exponential decay in hydraulic conductivity with depth on regional groundwater flow. *Geophysical Research Letters* **36** (24): 3–6 DOI: 10.1029/2009GL041251
- Jurgens BC, Böhlke JK, Eberts SM. 2012. An Excel® workbook for interpreting groundwater age distributions from environmental tracer data
- Jutebring Sterte E, Johansson E, Sjöberg Y, Huseby Karlsen R, Laudon H. 2018. Groundwater-surface water interactions across scales in a boreal landscape investigated using a numerical

modelling approach. *Journal of Hydrology* **560**: 184–201 DOI: 10.1016/J.JHYDROL.2018.03.011

Karlsen RH, Grabs T, Bishop K, Buffam I, Laudon H, Seibert J. 2016. Landscape controls on spatiotemporal discharge variability in a boreal catchment. *Water Resources Research* **52** (8): 6541–6556 DOI: 10.1002/2016WR019186

Kazemi GA, Lehr JH, Perrochet P. 2006. *Groundwater age*. Wiley-Interscience.

Klaminder J, Grip H, Mörth CM, Laudon H. 2011. Carbon mineralization and pyrite oxidation in groundwater: Importance for silicate weathering in boreal forest soils and stream base-flow chemistry. *Applied Geochemistry* **26** (3): 319–325 DOI: 10.1016/j.apgeochem.2010.12.005

Kolbe T, Marçais J, Thomas Z, Abbott BW, de Dreuzy J-R, Rousseau-Gueutin P, Aquilina L, Labasque T, Pinay G. 2016. Coupling 3D groundwater modeling with CFC-based age dating to classify local groundwater circulation in an unconfined crystalline aquifer. *Journal of Hydrology* **543**: 31–46 DOI: 10.1016/j.jhydrol.2016.05.020

Kozuskanich J, Simmons CT, Cook PG. 2014. Estimating recharge rate from groundwater age using a simplified analytical approach: Applicability and error estimation in heterogeneous porous media. *Journal of Hydrology* **511**: 290–294 DOI: 10.1016/J.JHYDROL.2014.01.058

Lagarias JC, Reeds JA, Wright MH, Wright PE. 1998. Convergence Properties of the Nelder--Mead Simplex Method in Low Dimensions. *SIAM Journal on Optimization* **9** (1): 112–147 DOI: 10.1137/S1052623496303470

Laudon H, Sjöblom V, Buffam I, Seibert J, Mörth M. 2007. The role of catchment scale and landscape characteristics for runoff generation of boreal streams. *Journal of Hydrology* **344** (3–4): 198–209 DOI: 10.1016/j.jhydrol.2007.07.010

Laudon H, Taberman I, Ågren A, Futter M, Ottosson-löfvenius M, Bishop K. 2013. The Krycklan

- Catchment Study — A flagship infrastructure for hydrology , biogeochemistry , and climate research in the boreal landscape. *Water resources Research* **49**: 7154–7158 DOI: 10.1002/wrcr.20520
- Ledesma JLJ, Futter MN, Blackburn M, Lidman F, Grabs T, Sponseller RA, Laudon H, Bishop KH, Köhler SJ. 2018a. Towards an Improved Conceptualization of Riparian Zones in Boreal Forest Headwaters. *Ecosystems* **21** (2): 297–315 DOI: 10.1007/s10021-017-0149-5
- Ledesma JLJ, Grabs T, Futter MN, Bishop KH, Laudon H, Köhler SJ. 2013. Riparian zone control on base cation concentration in boreal streams. *Biogeosciences* **10** (6): 3849–3868 DOI: 10.5194/bg-10-3849-2013
- Ledesma JLJ, Kothawala DN, Bastviken P, Maehder S, Grabs T, Futter MN. 2018b. Stream Dissolved Organic Matter Composition Reflects the Riparian Zone, Not Upslope Soils in Boreal Forest Headwaters. *Water Resources Research* **54** (6): 3896–3912 DOI: 10.1029/2017WR021793
- Leray S, de Dreuzay J-R, Bour O, Labasque T, Aquilina L. 2012. Contribution of age data to the characterization of complex aquifers. *Journal of Hydrology* **464–465**: 54–68 DOI: 10.1016/j.jhydrol.2012.06.052
- Leray S, Engdahl NB, Massoudieh A, Bresciani E, McCallum J. 2016. Residence time distributions for hydrologic systems: Mechanistic foundations and steady-state analytical solutions. *Journal of Hydrology* **543**: 67–87 DOI: 10.1016/j.jhydrol.2016.01.068
- Lindqvist G, Nilsson L, Gonzalez G. 1989. Depth of Till Overburden and Bedrock Fractures on the Svartberget Catchment as Determined by Different Geophysical Methods. *University of Luleå, Luleå, Sweden*: 16
- Maher K, Chamberlain CP. 2014. Hydrologic Regulation of Chemical Weathering and the

- Geologic Carbon Cycle. *Science* **343** (6178): 1502–1504 DOI: 10.1126/science.1250770
- Maloszewski P, Zuber A. 1996. Lumped parameter models for the interpretation of environmental tracer data (IAEA-TECDOC--910). International Atomic Energy Agency (IAEA)
- Marçais J, de Dreuzuy J-R, Erhel J. 2017. Dynamic coupling of subsurface and seepage flows solved within a regularized partition formulation. *Advances in Water Resources* **109**: 94–105 DOI: 10.1016/J.ADVWATRES.2017.09.008
- Marçais J, de Dreuzuy JR, Ginn TR, Rousseau-Gueutin P, Leray S. 2015. Inferring transit time distributions from atmospheric tracer data: Assessment of the predictive capacities of Lumped Parameter Models on a 3D crystalline aquifer model. *Journal of Hydrology* **525** (0): 619–631 DOI: <http://dx.doi.org/10.1016/j.jhydrol.2015.03.055>
- Mason BJ (ed.). 1991. *The surface waters acidification programme*. Cambridge University Press: Cambridge. DOI: 10.1017/CBO9780511600067
- McMahon PB, Plummer LN, Böhlke JK, Shapiro SD, Hinkle SR. 2011. A comparison of recharge rates in aquifers of the United States based on groundwater-age data. *Hydrogeology Journal* **19** (4): 779–800 DOI: 10.1007/s10040-011-0722-5
- Michaelides K, Chappell A. 2009. Connectivity as a concept for characterising hydrological behaviour. *Hydrological Processes* **23** (3): 517–522 DOI: 10.1002/hyp.7214
- Modica E, Buxton HT, Plummer LN. 1998. Evaluating the source and residence times of groundwater seepage to streams, New Jersey Coastal Plain. *Water Resources Research* **34** (11): 2797–2810 DOI: 10.1029/98WR02472
- Nyberg L. 1995. Water flow path interactions with soil hydraulic properties in till soil at Gårdsjön, Sweden. *Journal of Hydrology* **170** (1–4): 255–275 DOI: 10.1016/0022-1694(94)02667-Z

- Nyberg L, Stähli M, Mellander P-E, Bishop KH. 2001. Soil frost effects on soil water and runoff dynamics along a boreal forest transect: 1. Field investigations. *Hydrological Processes* **15** (6): 909–926 DOI: 10.1002/hyp.256
- Peralta-Tapia A, Sponseller RA, Ågren A, Tetzlaff D, Soulsby C, Laudon H. 2015a. Scale-dependent groundwater contributions influence patterns of winter baseflow stream chemistry in boreal catchments. *Journal of Geophysical Research: Biogeosciences* **120** (5): 847–858 DOI: 10.1002/2014JG002878
- Peralta-Tapia A, Sponseller RA, Tetzlaff D, Soulsby C, Laudon H. 2015b. Connecting precipitation inputs and soil flow pathways to stream water in contrasting boreal catchments. *Hydrological Processes* **29** (16): 3546–3555 DOI: 10.1002/hyp.10300
- Pinder GF, Celia MA. 2006. *Subsurface Hydrology*. Wiley.
- Pollock DW. 1988. Semianalytical computation of path lines for finite-difference models. *Ground Water* **26** (6): 743–750
- Renard P, Allard D. 2013. Connectivity metrics for subsurface flow and transport. *Advances in Water Resources* **51**: 168–196 DOI: 10.1016/J.ADVWATRES.2011.12.001
- Rodhe A. 1989. On the Generation of Stream Runoff in Till Soils. *Hydrology Research* **20** (1): 1–8 DOI: 10.2166/nh.1989.0001
- Schwarz M, Giadrossich F, Lüscher P, Germann PF. 2018. Subsurface hydrological connectivity of vegetated slopes: a new modeling approach. *Hydrology and Earth System Sciences Discussions*: 1–32 DOI: 10.5194/hess-2017-761
- Schwientek M, Maloszewski P, Einsiedl F. 2009. Effect of the unsaturated zone thickness on the distribution of water mean transit times in a porous aquifer. *Journal of Hydrology* **373** (3–4): 516–526 DOI: 10.1016/j.jhydrol.2009.05.015

Strack ODL. 1984. Three-Dimensional Streamlines in Dupuit-Forchheimer Models. *Water Resources Research* **20** (7): 812–822 DOI: 10.1029/WR020i007p00812

Troch P, van Loon E, Hilberts A. 2002. Analytical solutions to a hillslope-storage kinematic wave equation for subsurface flow. *Advances in Water Resources* **25** (6): 637–649 DOI: 10.1016/S0309-1708(02)00017-9

Visser A, Broers HP, Heerink R, Bierkens MFP. 2009. Trends in pollutant concentrations in relation to time of recharge and reactive transport at the groundwater body scale. *Journal of Hydrology* **369** (3–4): 427–439 DOI: 10.1016/J.JHYDROL.2009.02.008

Vogel JC. 1967. Investigation of groundwater flow with radiocarbon. In: IAEA (Ed.), *Isotopes in Hydrology*. IAEA, Vienna, p. 15

Tables

Tab. 1: Summary of model results for simulations with different infiltration rates I and the resulting distance to the steam within subsurface discharge occurs L_d , the groundwater recharge to the deeper less permeable layer $R_{deep\ layer}$, mean groundwater age at sampling locations τ_w , lag of rejuvenation τ_d (mean groundwater age related to the discharge zone) as well as mean groundwater age related to the recharge zone τ_r .

Simulation	I [mm/a]	L_d [m]	$R_{deep\ layer}$ [mm/a]	τ_d [a]	τ_r [a]	τ_w [a]
Reference	321	240	109 (34% of total)	36	28	64
Winter	146	95	94 (64% of total)	14	46	60
Spring	840	340	177 (21% of total)	42	21	63

Figure Legends

Fig. 1: Location of the Svartberget study site in northern Sweden (a) with its topography (b) its soil types (c) and the tree volume (d).

Fig. 2: From the Svartberget catchment (inset to the left), we extracted a representative hillslope with elevation (solid black line) plotted against the distance to the stream. Also plotted are the interface between the shallow permeable and deeper less permeable layer (black, dashed line), the bottom of the aquifer (black, dotted line) as well as the width of the hillslope (blue, dashed line) and the fitted width (blue solid line). The elevations of sampling locations are marked with open circles at the respective distances of the sampling from the stream.

Fig. 3: Measured CFC-based groundwater age stratification left and sampling locations right.

Fig 4: Groundwater age stratification within the area of sampling locations (circles, numbers indicate distances to the stream). Modeled groundwater ages are shown within the distances of 80 m to 20 m to the stream. The 20 m distance is shown in grey, transitioning to the 80 m distance in copper.

Fig 5: Distribution of groundwater ages within the representative hillslope. The red line shows the interface between the shallow permeable layer and deeper less permeable layer. The red dashed line indicates the locations at which recharge to the aquifer takes place. The red continuous line indicates the extent of the subsurface discharge zone.

Fig 6: A. Graphical presentation of the representative hillslope and generation of the discharge zone in the discharge area. B. Presentation of the idealized aquifer and mean groundwater ages. C. Measured groundwater ages versus depth and derived mean groundwater ages.

Fig 7: A. Groundwater age stratifications within the distances of 80 m to 20 m to the stream are shown for different recharge rates (blue: winter model, red: reference model, green: spring model).

B. Water table locations for the winter model (blue), the reference model (red) and spring model (green). The dashed line represents the interface between the shallow permeable layer and the deep less permeable layer. The dotted line shows the aquifer bottom.

Accepted Article

Appendix

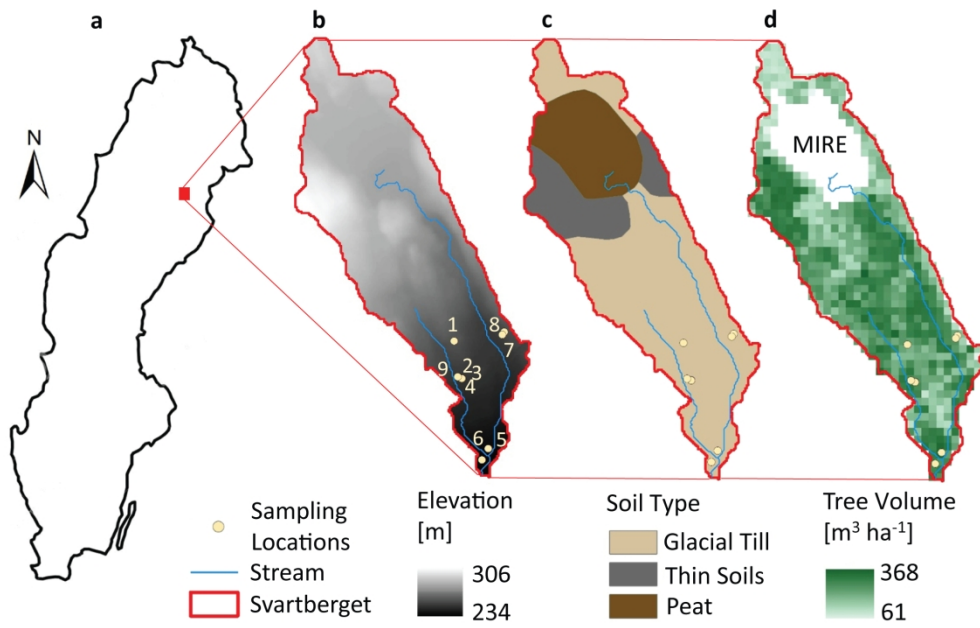
Tab. A1: Measured CFC concentrations and derived groundwater ages for the 9 sampling locations within the Svartberget study site.

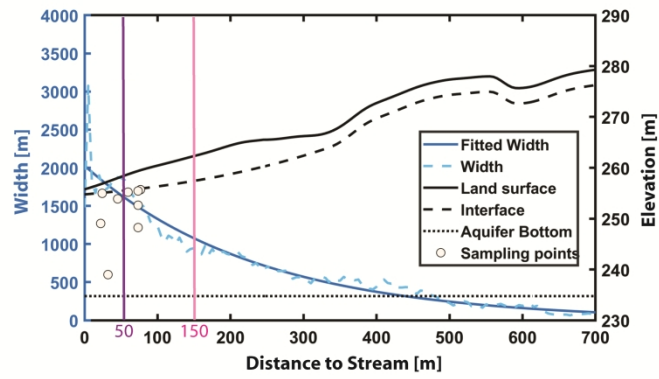
ID	Sampling interval below water table [m]	Unsaturated zone thickness [m]	CFC-12 [pptv]	CFC-12 based groundwater age [a]	CFC-11 [pptv]	CFC-11 based groundwater age [a]	CFC-113 [pptv]	CFC-13 based groundwater age [a]
1	0-0.4	2.6	423.2	30	170.0	37	52.7	31
2	0-0.8	1.5	414.5	31	133.7	41	47.1	31
3	2.7-3.7	1.5	341.5	35	15.4	55	17.8	39
4	7.1-8.1	2.2	238.5	42	62.0	47	27.3	36
5	5.5-6.5	2.7	43.1	56	14.0	55	4.5	49
6	15.7-16.7	1.18	57.8	54	13.8	56	1.4	57
7	0-0.7	1.9	400.5	31	161.1	38	51.4	31
8	1-2	1	358.4	34	118.8	42	29.2	35
9	0-0.2	0.9	378.4	33	170.3	37	63.1	29

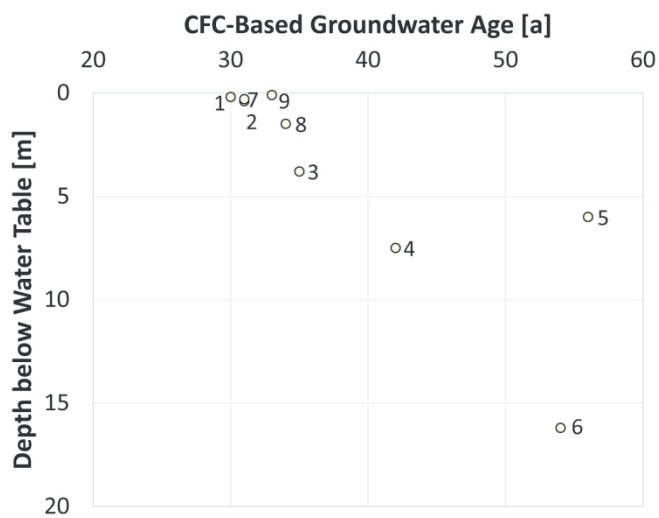
Sampling locations 1, 2, 3, 7, 8, and 9 show similar CFC-12 and CFC-113 based groundwater ages with much higher CFC-11 based groundwater ages. This pattern indicates effects of microbial degradation on CFCs in the aquifer which lead to a degradation of CFC-11 (IAEA, 2006). Sampling locations 4 and 5 show differences of a few years by comparing CFC-based groundwater ages (less than 7 years), whereas for sampling location 6 the CFC-based groundwater ages coincide.

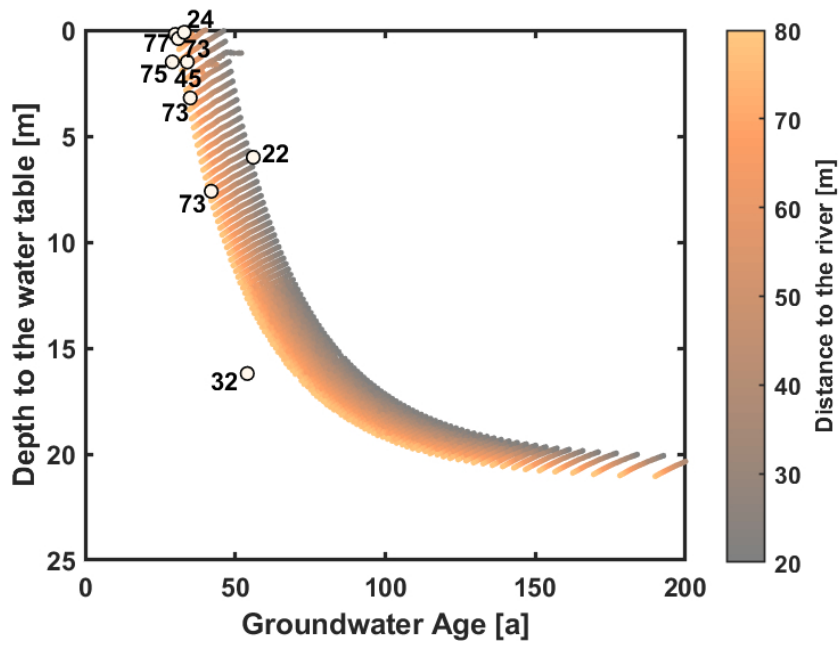
Tab. A2: Modelled and measured CFC-12 concentrations for each of the 9 sampling locations. The mean residence and mean travel distance of the particles reaching the sampling locations are derived from the calibrated model. The apparent groundwater age is determined from measured CFC-12 concentrations.

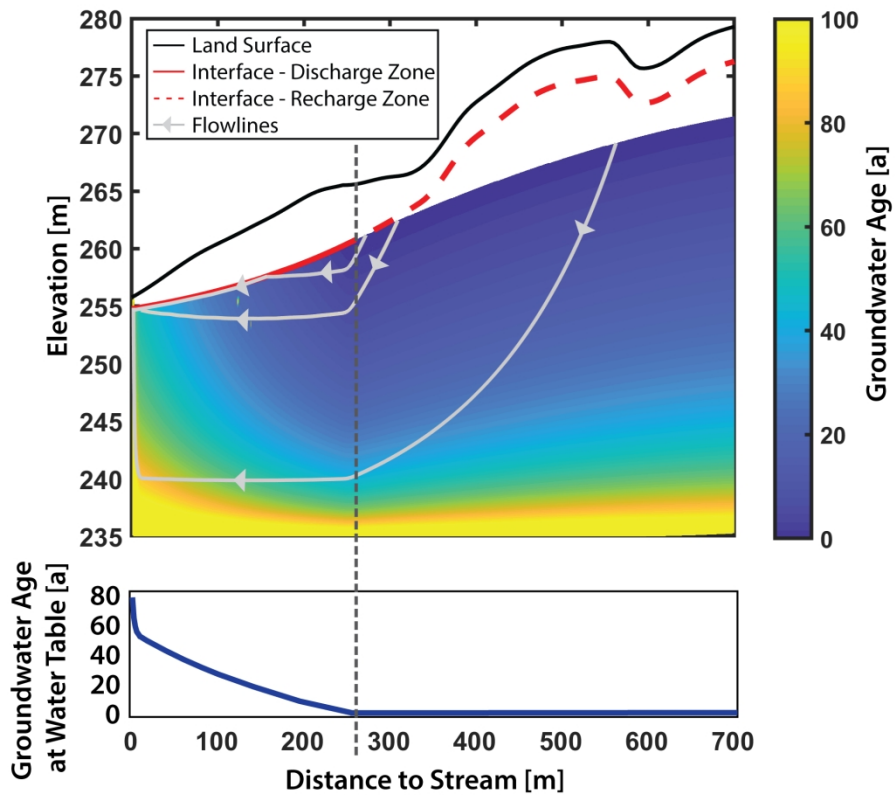
ID	CFC- 12 modelled [pptv]	CFC-12 measured [pptv]	Mean residence time (modelled) [a]	Apparent groundwater age [a]	Mean travel distance [m]
1	429	423	28	30	206
2	416	415	30	31	215
3	376	342	33	35	247
4	300	239	40	42	306
5	207	43	51	56	346
6	67	58	84	54	564
7	383	401	33	31	229
8	329	358	38	34	259
9	282	378	42	33	275

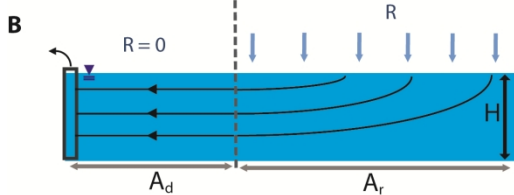
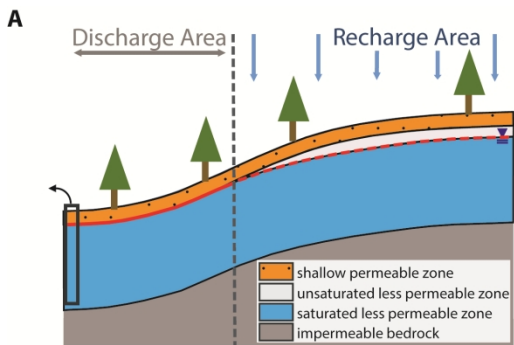












$\tau_w = \tau_d + \tau_r$
$\tau_w = \frac{\Phi H A_d}{R A_r} + \frac{\Phi H}{R}$

